Pergamon

0301-9322(95)00018-6

Int. J. Multiphase Flow Vol. 21, No. 5, pp. 775–785, 1995

0301-9322/95 $9.50 + 0.00

PARTICLE STRESS AND VISCOUS COMPACTION DURING SHEAR OF DENSE SUSPENSIONS

D. PRASAD and H. K. KYTÖMAA†

Department of Mechanical Engineering, Massachusetts Institute of Technology, Cambridge, MA 02139, U.S.A.

(Received 22 September 1994; in revised form 26 February 1995)

Abstract—This study describes the transition between the quasi-static and the viscous regimes of shearing of thin layers of spheres in a viscous fluid at high solid loadings. Experiments were conducted in a Couette-type shear cell in two complementary modes: (a) constant particle normal stress, variable solid fraction and (b) constant solid fraction, variable particle normal stress. During steady shearing under the constraint of constant solid fraction, transition from a strain rate independent stress to one with a linearly dependent behavior was found to occur with a local minimum in the stresses with respect to strain rate; correspondingly, the solid fraction assumed a maximum with respect to strain rate under conditions of constant normal stress. These are the first observations of such a phenomenon, which we call viscous compaction. At sufficiently high strain rates, the mixture exhibited a linear Newtonian-like scaling between strain rate and both shear and normal stresses. These measurements of normal stress are the first since those of Bagnold.

Key Words: dense suspensions, viscous interaction, transition

1. INTRODUCTION

Dense suspensions of solid particles in Newtonian fluids are frequently encountered in natural and industrial flows. In the case of flows such as avalanches and landslides, the granular material may fail dramatically, causing a flow to occur with catastrophic consequences. In the processing of ceramics and in powder metallurgy, for instance, materials in the finely divided state have to be handled at the maximum possible solid fraction; simultaneously, it is essential that these slurries have good mobility which is difficult to attain. Consequently, it is important to understand the physical phenomena peculiar to these mixtures in order to better predict their flows.

Suspension flows may be broadly classified as belonging to one of three regimes: quasi-static, viscous or inertial. Reynolds (1885) showed that a saturated non-Brownian suspension in a random close packed (RCP) configuration must dilate under shear to sustain continued deformation. This phenomenon is called Reynolds dilatation. At extremely low strain rates and under the application of a normal force, strain rate independent stresses are set up in the medium (Bridgewater 1972; Buggisch & Stadler 1986). This is the quasi-static regime and it is dominated by short-range frictional interactions between the particles resulting from extended contact. Consequently, models based on Coulomb interactions have been successfully applied to describe the slow flow of grain in hoppers (Brennen & Pearce 1978; Nguyen *et al.* 1979) and the mechanics of soils (Scott 1963; Schofield & Wroth 1968).

As the strain rate is increased, it is to be expected that the interstitial fluid will play an increasingly important role and at sufficiently high strain rates, fluid viscosity will govern the behavior of the mixture. This regime was first studied systematically by Bagnold (1954) who showed that both the shear and normal stress (τ and σ respectively) scale linearly with $\lambda^{3/2}\mu\dot{\gamma}$ where λ is the ratio of particle diameter to mean (surface-to-surface) spacing between neighbors, μ is the fluid viscosity and $\dot{\gamma}$ is the strain rate. This linear dependence of τ on $\dot{\gamma}$ has prompted the appellation viscous regime. Later studies by Cheng & Richmond (1978), Gadala-Maria & Acrivos (1980), Thomas (1965), Rutgers (1962) and Pätzold (1980), amongst others, have demonstrated the inaccuracy of

†Present address: Failure Analysis Associates, 3 Speen St, Framingham, MA 01701, U.S.A.

Bagnold's scaling for the shear stress; all of the reliable experimental data show that τ scales with $\lambda\mu\dot{\gamma}$ (Frankel & Acrivos 1967). However, no measurements of normal stress exist other than those of Bagnold. In fact, several theoretical studies (Leighton & Acrivos 1987; Brady & Bossis 1985) have suggested that a normal stress cannot be generated in Newtonian suspensions in the absence of particle contact. In addition, the investigation of Cheng & Richmond (1978) has been the only one since that of Bagnold to examine the behavior of suspensions very close to maximum packing. One of their unexpected discoveries was that in the case of 'coarse materials', the shear stress is a decreasing function of strain rate, a phenomenon that they attributed to changes in the packing density.

At still higher values of strain rate, the flow enters the inertial regime which is dominated by collisional interactions between the particles resulting in momentum exchange in a manner akin to the molecules of a dilute gas. This regime was first discovered by Bagnold (1954) who showed that the generated normal and shear stresses scale with $\lambda\dot{\gamma}^2$. This has since been confirmed experimentally (Savage & McKeown 1978; Savage & Sayed 1984; Hanes & Inman 1985), numerically (Campbell & Brennen 1985; Hopkins & Louge 1991) and kinetic theories have also been developed that are successful in predicting the qualitative behavior of these mixtures (Jenkins & Savage 1983).

The transition from the viscous to the inertial regime was examined by Bagnold and manifests itself as a change from a linear scaling of stress with respect to strain rate to a quadratic one and is well understood. In contrast, the nature of the transition from the quasi-static to the viscous regime remains unclear despite its important implications in events associated with the loss or gain of shear strength of a granular assembly such as flow failures and pipe blockage.

The present investigation addresses this transition and aims to understand the scaling of the stresses in the transitional and viscous regime. Of particular interest is the behavior of the normal stress in the viscous regime, if it exists. In all of the data presented, the size of the symbols is representative of the experimental error, unless otherwise indicated.

2. APPARATUS

The experiments were conducted using a dynamic shear cell which provides the capability of conducting steady and transient shear experiments with solid–liquid mixtures at large volumetric

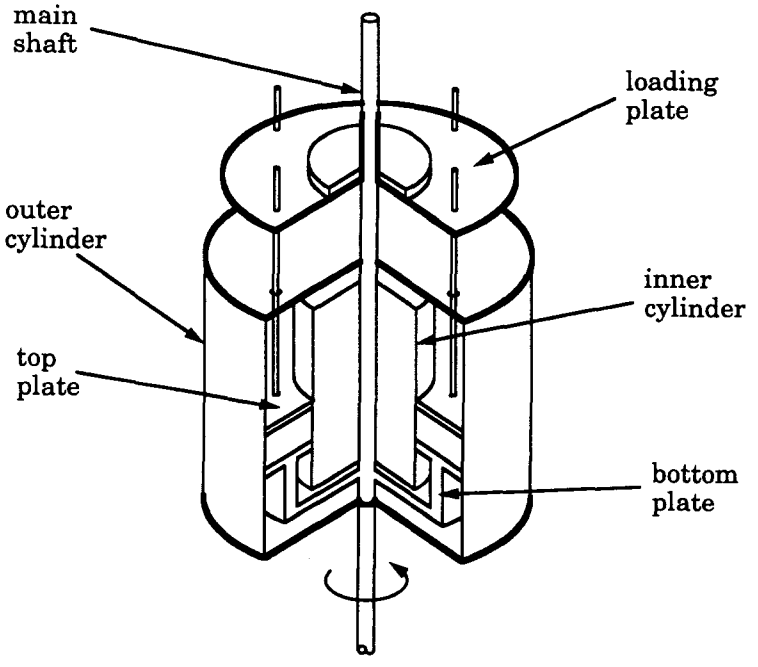

Figure 1. The dynamic shear cell: schematic view.

solid fractions, upto and including maximum packing configurations. The apparatus is described in detail by Poutiatine (1990) and by Prasad (1993). The arrangement is shown schematically in figure 1. The mixture is confined within the annular space between two coaxial vertical cylinders with nominal diameters of 0.219 and 0.435 m. Shearing takes place between a pair of horizontal plates that span the annular gap. The bottom plate rotates and the stresses are measured at the top plate, which is specially designed to measure the stresses generated in the particle matrix alone.

Reynolds dilatation occurs when a compact granular assembly is sheared from rest. If the mixture is confined to a fixed volume with impervious walls (as is the case in conventional viscometers), the following situation arises: the particle matrix is prevented from undergoing dilatation, resulting in a generation of normal stress, which causes a decrease in the net volume of solids due to Hertzian interactions. Consequently, a partial vacuum may be generated in the fluid notwithstanding the presence of a compressive stress state in the solid phase. Thus a normal stress that is measured at the impermeable wall would be ambiguous as it can result from a combination of a compressive solid stress and a tensile fluid stress. The top plate of the shear cell is therefore made porous; this allows the pore pressure to equilibrate across the wall and the stress that is measured results solely from the coupling of the particulate medium and the wall.

Additionally, the seal between the wall and the top plate is of a non-contact knife-edge type so that the entire top plate is free to rotate about the vertical axis and translate along it. The upper wall, made of acrylic, is rough; it is perforated with cylindrical 4 mm diameter holes 1.8 mm deep that cover 55% of the surface. It was observed that the particles tended to partially lie in and protrude from these holes. The bottom rotating wall was covered with a thin layer of silicon rubber in which 2 mm glass spheres were embedded at a mean spacing of 5 mm. Thus both surfaces were rough with a roughness scale of the order of the particle diameter. The particles used were 3.175 mm acrylic spheres and 2 mm glass spheres. Glycerol–water mixtures in varying concentrations were used as interstitial fluids. A thermostat coupled with an on–off controller was used to control the flow of chilling water around the periphery of the shear cell to ensure that the mixture temperature and hence the fluid viscosity remained constant.

The apparatus was designed so that the bottom plate is capable of both steady as well as oscillatory rotation. The test procedure began with a measured mass of particles being placed in the shear cell. The interstitial fluid was then poured in and an oscillatory motion was imparted to the mixture via the bottom plate until it became uniform. The top plate was then lowered onto the mixture. This procedure ensured consistency in the experimental runs. The maximum solid fraction achieved at rest did not differ from that observed during the shearing tests.

Two kinds of experiments were conducted. The first consisted of imposing a normal stress with weights or by means of partially levitating the top plate using a pneumatic actuator; in this mode the top plate was free to move vertically and the mixture was allowed to assume an equilibrium solid fraction which was measured. The shear stress was calculated by measuring the restraining torque necessary to hold the top plate in position.

In the second type of experiment, the volume occupied by the solid phase was held fixed by locking the top plate axially. In this instance, both the normal and shear stresses were measured directly using a floating element of rough wall (diameter 83 mm) connected to a two-dimensional force balance shown in figure 2. A more detailed description is given in a later section.

In both types of experiments, the total volume of particles in the shear cell was such that the length scale of the region of shear was approximately 10 particle diameters at the largest solid fractions. It is well known from studies using larger numbers of particle layers (Hanes & Inman 1985; Thompson & Grest 1991) that the thickness of the shear band is 10–15 particle diameters and moreover, that the strain rate is nearly uniform across this band. Thus, in the present experiments, shearing takes place over a length scale that is of the order of a typical shear band. It is therefore reasonable to expect that the strain rate is uniform. In addition, some limited visual observations through a viewport in the side of the shear cell showed that there were no locked zones present.

3. EXPERIMENTS AT CONSTANT NORMAL STRESS

Experiments at constant normal stress were conducted using 2 mm glass spheres and a water–glycerol mixture with a viscosity of 35×10^{-3} kg m^{-1}s^{-1}. The shear stress, τ, and (volumetric)

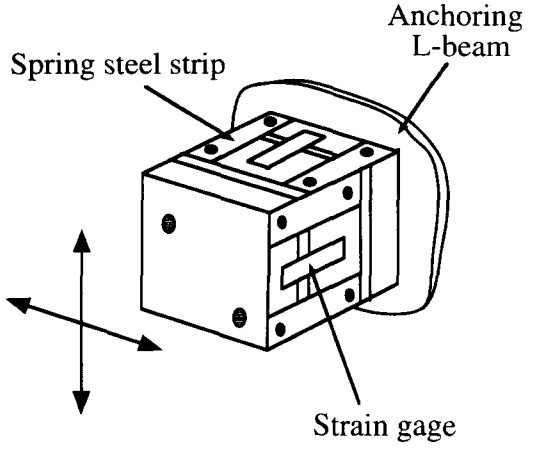

Figure 2. Force balance used in the direct measurement of the shear and normal stresses.

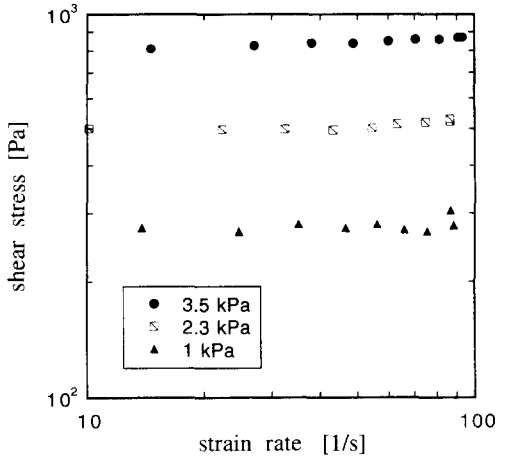

Figure 3. Dependence of τ on $\dot{\gamma}$ under conditions of constant σ.

solid fraction, ϕ, were measured after steady state was attained for each value of the normal stress, σ, and strain rate, $\dot{\gamma}$. Long time records showed no slow variations. The behavior was also found to be non-hysteritic in strain rate.

Figure 3 shows the behavior of τ as a function of σ and $\dot{\gamma}$. There appears to be little dependence on strain rate, particularly at larger σ. This is in agreement with the data of Bridgewater and Buggisch & Stadler as well as those of Hungr & Morgenstern (1984). A similar strain rate independence was observed in the simulations of Thompson & Grest (1991).

The measured ϕ under conditions of constant σ, shown in figure 4, behaved in an unexpected manner. As $\dot{\gamma}$ was increased from its lowest value, ϕ was found to increase and then decrease rather than decrease monotonically as would be the case for viscous (Bagnold) dilatation or remain constant, as in quasi-static shearing. Furthermore, increasing σ has the effect of shifting the solid fraction curve upward. Traditionally, the maximum packing fraction, ϕ_m is defined for sheared granular assemblies as that value of ϕ above which the medium cannot be sheared and has been assumed to be a constant (Frankel & Acrivos 1967). However, from figure 4, it is clear that the peak solid fraction achieved at a given value of σ may be regarded as a maximum solid fraction corresponding to that σ. Hence, ϕ_m is not a constant but rather a function of σ. This variation of ϕ_m with σ has been demonstrated by Onoda & Liniger (1991) in the limit of vanishing σ. In their experiments, the stress state of the sheared medium was controlled by varying the degree of

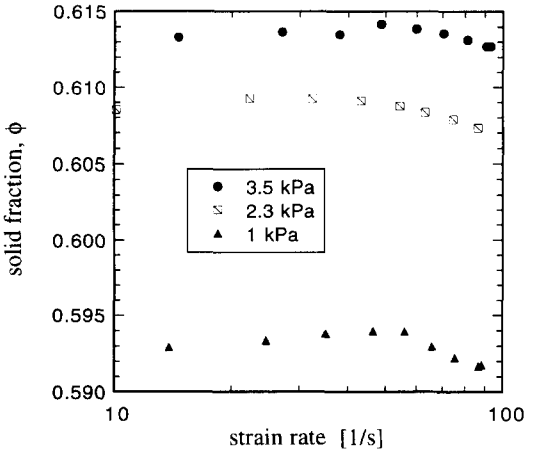

Figure 4. ϕ as a function of $\dot{\gamma}$ with σ held constant.

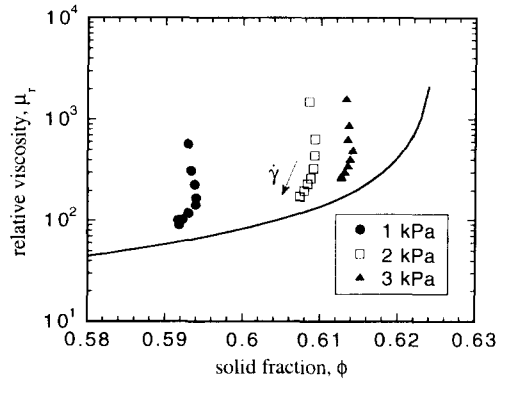

Figure 5. Relative viscosity as a function of ϕ at constant imposed normal stress. The symbols represent the present experimental data; the solid line represents the theoretical curve of Frankel & Acrivos (1967).

mismatch between the solid and liquid phases in the presence of gravity. They found a monotonic increase in ϕ above $55 \pm 1\%$ with σ where the latter concentration is the so-called stress percolation limit below which σ disappears. For mixtures at high solid loadings, the meaning of a maximum packing becomes ambiguous and for a monodisperse mixture, it has been shown to assume a value anywhere between the above stress percolation limit and the random close pack limit of $63 \pm 1\%$ (Scott 1960; Finney 1970; Savage & McKeown 1983).

The relative viscosity, $\mu_r = \tau/(\mu\dot{\gamma})$ is plotted against ϕ in figure 5. σ is held constant along each curve. For comparison, the theoretical curve of Frankel & Acrivos, which is known to agree with numerous experimental measurements of dense suspensions, is also plotted; it is given by

$$\mu_r = C\left[\frac{1}{(\phi_m/\phi)^{1/3} - 1}\right]$$

where C is a constant. In the present case the value of ϕ_m used was 0.63. Figure 5 shows that the measured values of μ_r tend toward the Frankel–Acrivos curve with increasing strain rate.

One puzzling observation during these experiments was that the system underwent large oscillations at low values of $\dot{\gamma}$. These oscillations were violent enough to cause breakage of the particles and disappeared when the strain rate was increased. Similar behavior has been reported in the past by other investigators (Cheng & Richmond 1978; Savage & McKeown 1978). It turns out that these oscillations have an interesting fundamental explanation which is the subject of another paper (Prasad & Kytömaa 1995).

The above experiments identify a phenomenon of compaction which arises as the mixture is sheared sufficiently fast at constant normal stress. It is believed to reflect the onset of viscous effects and for this reason, the phenomenon may be called viscous compaction.

4. EXPERIMENTS AT CONSTANT SOLID FRACTION

4.1. Experimental details

With a view to eliminating the unsteady oscillations observed in the constant normal stress study, further experiments were conducted in a true strain rate controlled configuration. To this end, the top plate assembly was stiffened and locked axially along the main shaft.

The stresses were measured directly by means of a circular floating element of wall that was cut out of the top plate and connected to a two-dimensional force balance. The narrow gap between the floating element and the rest of wall was restricted to a size of 1 mm to prevent particles from jamming into the gap. The force balance consists of three aluminum blocks, cantilevered together in mutually perpendicular directions using spring steel strips as stiffness elements and the deflections are measured by means of strain gages (see figure 2). The assembly was done with great care to ensure that the shear and normal deformations were truly independent.

In this series of experiments, the aim was to observe the behavior of the system over a wide range of normal stress. Hence, it was imperative that the density mismatch between the interstitial fluid and the particles be minimal in order to reduce the variation of σ across the height of the bed. The particles used were 3.175 mm acrylic spheres with a size distribution shown in figure 6. The interstitial fluid used was an aqueous solution of glycerol with a viscosity of $70 \times 10^{-3}\,\mathrm{kg\,m^{-1}\,s^{-1}}$. The mixture was subjected to steady shearing and the shear stress, normal stress and driving rpm signals were input to a data acquisition system and averaged. In these experiments, the Reynolds number based on the particle diameter and the mean speed of the moving wall ranged from unity to about 35 while the Bagnold number was calculated to lie between 0.25 and 12. The small values of both parameters reflect the extreme slowness of the shearing.

4.2. Stress–strain rate scaling

It was shown earlier that under conditions of constant σ, ϕ assumes a maximum at a critical strain rate $\dot{\gamma}$ and that an increase in σ shifts the curve upward in ϕ. As shown in figure 4, the experiments were conducted at three values of σ. Based on these data, it is to be expected that the dependence of ϕ on σ and $\dot{\gamma}$ will appear as shown schematically in figure 7(a). If a horizontal line is drawn across this plot, representing a test carried out at constant ϕ, it will first encounter lines

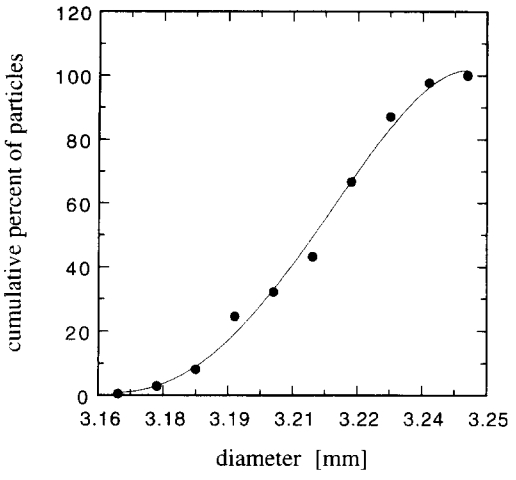

Figure 6. Size distribution of the acrylic spheres used in the constant solid fraction experiments.

of decreasing σ; after a minimum value of σ is reached, the trend is reversed and lines of increasing σ are encountered. At constant ϕ, the normal stress σ is therefore expected to possess a minimum with respect to strain rate as shown in figure 7(b).

The measured σ and τ are plotted in figure 8(a) and (b) as functions of $\dot{\gamma}$ with ϕ as a parameter. While the experiments were conducted over a wide range of ϕ, only a few representative values are shown to clarify the behavior of the suspension. These measurements are the first since those of Bagnold to directly measure the normal stress in a sheared suspension. Moreover, as discussed earlier, they are the only unambiguous measurements of σ in the dispersed phase since the stresses in the fluid phase are permitted to equilibrate.

For low values of ϕ, both τ and σ exhibit a monotonic increase with $\dot{\gamma}$. With increasing ϕ, evidence of quasi-static behavior is apparent; both stresses exhibit weak strain rate dependence at low strain rates. At higher $\dot{\gamma}$, the suspension recovers its linear dependence on $\dot{\gamma}$. At still higher values of ϕ, σ exhibits a local minimum with $\dot{\gamma}$, as anticipated; correspondingly, τ also exhibits a local minimum at the same value of $\dot{\gamma}$. The most interesting feature is the reduction in the stresses with increasing $\dot{\gamma}$. A possible mechanism for this is as follows. The interstitial fluid is squeezed due to relative motion between the particles and as $\dot{\gamma}$ increases, lubrication interactions assume an increasing importance. Once lubrication between the particles becomes increasingly important, it may be expected that the shear and normal forces will be significantly reduced compared with the forces of solid–solid interaction. This reduction in τ and σ would continue until lubrication is the dominant interaction. Further increase in $\dot{\gamma}$ would then cause an increase in τ and σ which would ultimately scale linearly with $\dot{\gamma}$ at high strain rates. The present observations are in qualitative agreement with the results of Cheng & Richmond described earlier in this paper where the authors report a decreasing τ–$\dot{\gamma}$ relationship; however, their measurements were limited to one value of ϕ which was not recorded and a limited range of $\dot{\gamma}$ so that the local minimum in shear stress was not observed.

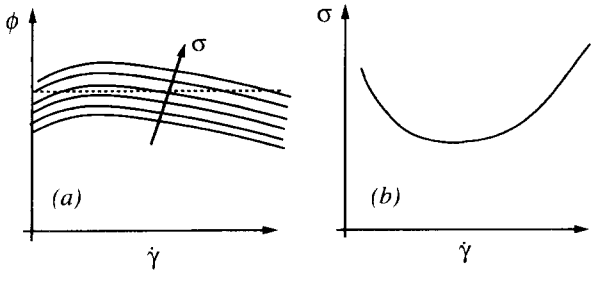

Figure 7. (a) Schematic representation of ϕ as a function of $\dot{\gamma}$ at constant σ; (b) expected behavior of σ as a function of $\dot{\gamma}$ at constant ϕ.

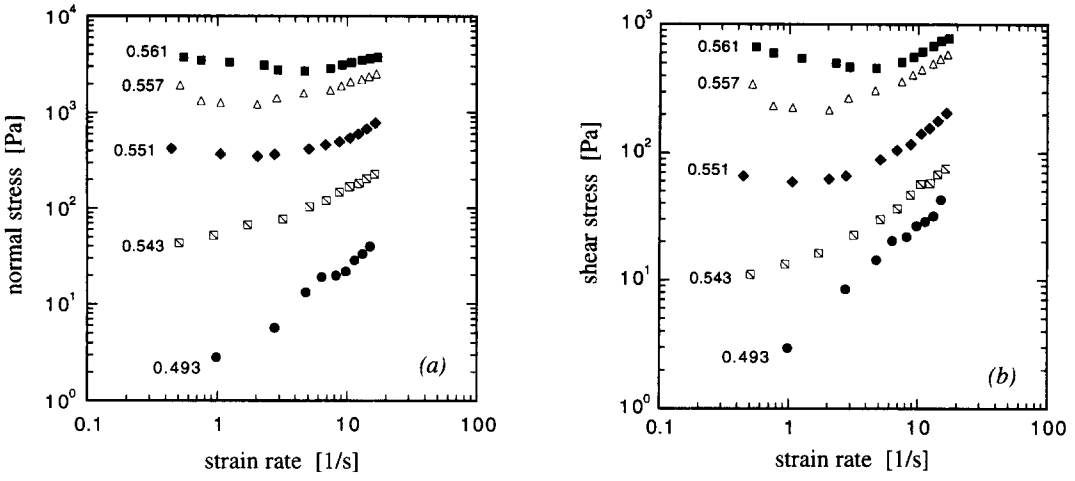

Figure 8. (a) Normal stress and (b) shear stress as functions of $\dot{\gamma}$ at constant ϕ.

The presence of a local minimum in the τ–$\dot{\gamma}$ relationship has important implications on the stability of conventional rheometric systems which are generally used in shear stress measurements of suspensions and do not incorporate a floating element of wall, unlike the present device. When τ is a decreasing function of $\dot{\gamma}$, it may be shown (Prasad & Kytömaa 1995) that the system is linearly unstable; a full non-linear analysis indicates that it will undergo a large scale limit cycle behavior with sudden accelerations and decelerations. It is believed that this instability was responsible for the large scale oscillations observed during the constant normal stress experiments.

4.3. Relative viscosity

The relative viscosity, μ_r is plotted in figure 9 as a function of $\dot{\gamma}$ and ϕ. At low strain rates and high solid fractions, the curves have a slope near -1, indicating a constant shear stress. At $\phi = 0.491$, μ_r is constant with strain rate, reflecting the linear shear stress scaling with strain rate. At high ϕ, the curves appear to asymptote to a constant value although they do not quite flatten.

The maximum strain values of μ_r are plotted against ϕ in figure 10. The theoretical curve of Frankel & Acrivos is also plotted for comparison. The value of the maximum packing fraction required in the Frankel–Acrivos expression was determined using the procedure suggested by Thomas which consists of plotting $[\mu_r - 1]^{-1}$ and extrapolating to zero ordinate; the value obtained was 0.562. From figure 10, it is clear that the present data are in qualitative agreement with earlier

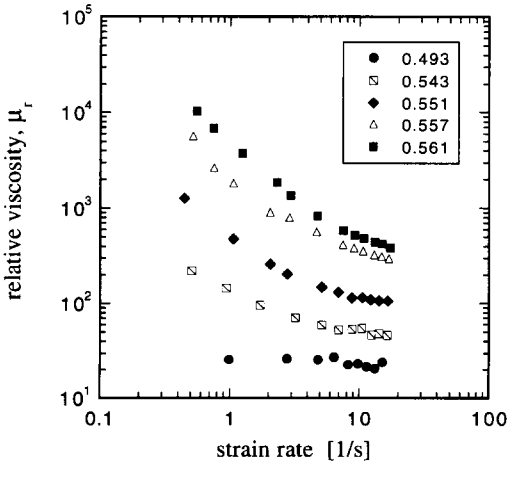

Figure 9. Relative viscosity μ_r as a function of $\dot{\gamma}$: ϕ is held constant along each curve.

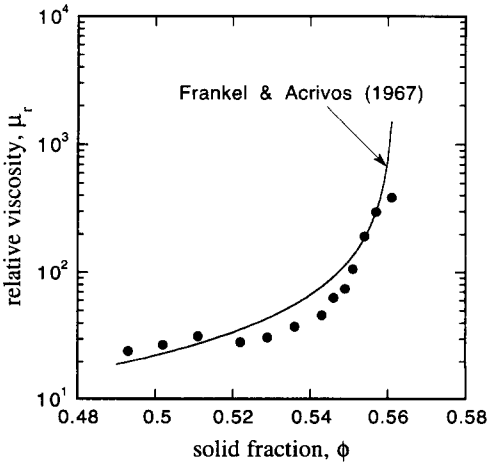

Figure 10. Asymptotic values of μ_r in figure 9 as a function of ϕ.

results despite the fact that the present measurements have not reached their high $\dot{\gamma}$ asymptotic values.

4.4. *Shear–normal stress ratio*

The ratio τ/σ is an indicator of the nature of the interactions between the particles. At very low solid fractions, one might expect that particle–particle interaction is minimal so that no normal stress is generated, yielding $\tau/\sigma \to \infty$. Conversely, at large ϕ and low $\dot{\gamma}$, particle friction would be the dominant interaction and τ/σ can be expected to approach the coefficient of dynamic Coulomb friction.

Figure 11 shows the ratio τ/σ as a function of $\dot{\gamma}$ and ϕ. Despite the scatter in the data, a weak dependence on $\dot{\gamma}$ is suggested. In addition, the curves appear to asymptote to a constant τ/σ. The values of τ/σ at the maximum $\dot{\gamma}$ are plotted as a function of ϕ in figure 12. An exponential falloff with ϕ seems evident. That τ/σ should increase with increasing dilution is intuitively correct since σ much vanish as $\phi \to 0$. In contrast, Bagnold found that τ/σ remained constant in the viscous regime at 0.75; however, his tests were conducted at only one value of ϕ. It must be emphasized that the curves in figure 11 have not yet reached their asymptotic values at the maximum strain rate so that the dependence of τ/σ on ϕ in figure 12 could very possibly flatten out at large ϕ.

4.5. *Influence of fluid viscosity*

In order to investigate the dependence of the transition on interstitial fluid viscosity, additional experiments were conducted using a fluid with a viscosity one order of magnitude lower than that used in the earlier tests. A glycerol–water mixture of viscosity $55 \times 10^{-4}\,\mathrm{kg\,m^{-1}\,s^{-1}}$ was used. Due to the severe mismatch of density between the two phases, the experiments were carried out only at very high solid fractions.

Figure 13(a) and (b) shows the shear and normal stress scaling in comparison with the earlier data. Since lubrication forces scale with fluid viscosity, it is to be expected that quasi-static behavior should be exhibited more persistently than in the earlier experiments. This is indeed the case; in figure 13(a) and (b), the $\phi = 0.554$ curves for τ and σ are still falling at low $\dot{\gamma}$ when $\mu = 55 \times 10^{-4}\,\mathrm{kg\,m^{-1}\,s^{-1}}$ whereas the corresponding curves with $\mu = 70 \times 10^{-3}\,\mathrm{kg\,m^{-1}\,s^{-1}}$ have already started increasing at the same $\dot{\gamma}$. Additionally, at low $\dot{\gamma}$, the stresses are the same for both sets of experiments, indicating a weak dependence on μ, which might be expected in a Coulomb friction dominated regime.

However, figure 13(a) and (b) shows that the $\dot{\gamma}$ at which the minimum in the stress curves occurs is not influenced by μ to any significant extent. This is somewhat counterintuitive since one would expect this parameter to be dependent on μ if the transition is a lubrication phenomenon. At present, the reason for this is not clear.

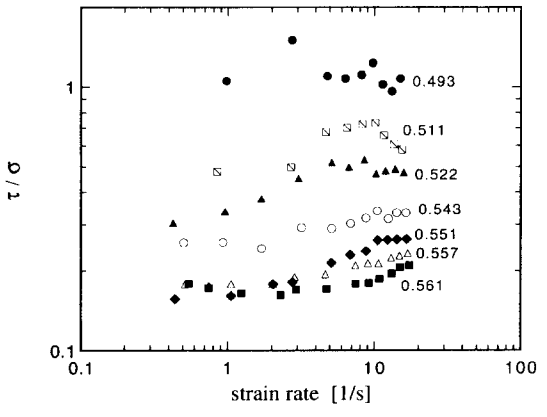

Figure 11. Ratio of shear to normal stress (τ/σ) as a function of $\dot{\gamma}$ under conditions of constant ϕ.

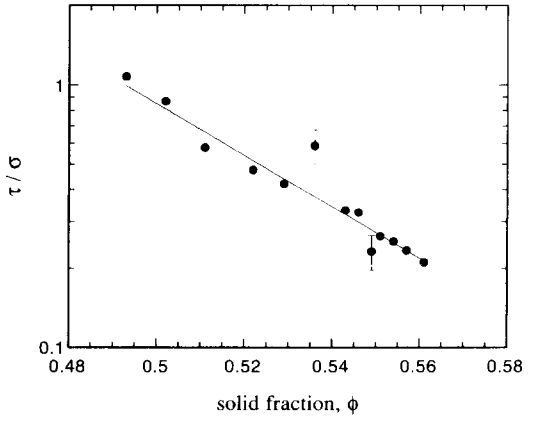

Figure 12. Scaling of the asymptotic value of τ/σ in figure 11 with ϕ.

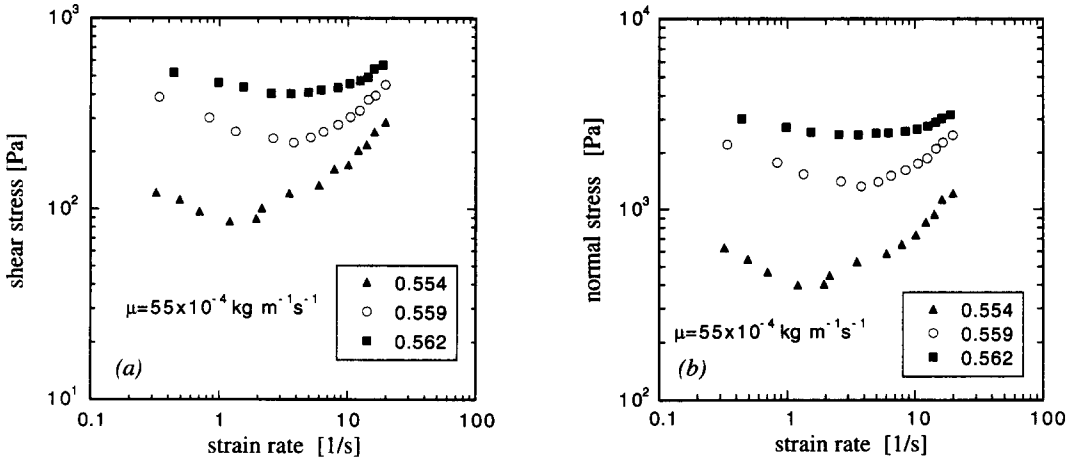

Figure 13. (a) Shear stress and (b) normal stress as functions of $\dot{\gamma}$ at constant ϕ with a reduced fluid viscosity.

4.6. *Maximum packing fraction*

This parameter is often defined as that solid fraction at which the mixture cannot be sheared; it is a function of the internal microstructure. Consequently, changes in the microstructure are manifested as variations in the maximum packing fraction. The minimum normal stress is plotted as a function of solid fraction in figure 14. This can also be interpreted as the maximum packing achieved at the corresponding imposed normal stress. In figure 14, data were used only from τ–$\dot{\gamma}$ curves that had a definite minimum. The extreme sensitivity of ϕ_m to normal stress is apparent as might be expected from the normal stress curves in figure 8(a). The present data complement those of Onoda & Liniger whose experiments were conducted in the limit of $\sigma \to 0$. Here, the large σ limit is investigated.

The curve in figure 14 appears to asymptote to $\phi \sim 0.565$. It is speculated that higher solid fractions may be achieved at large σ through phase transitions which would be manifested as discontinuous jumps in ϕ. Further, ϕ_m appears to fall off exponentially as σ is decreased from large values and this is consistent with the relationship between τ/σ and ϕ shown in figure 12.

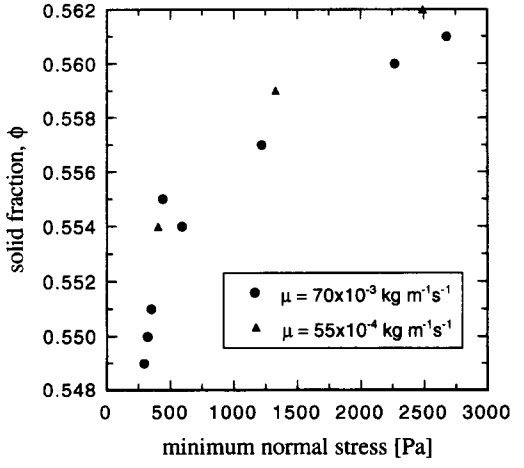

Figure 14. The minimum normal stress achieved during constant ϕ experiments as a function of ϕ and fluid viscosity.

5. CONCLUSION

Experiments were conducted to study the transition between the quasi-static (solid friction dominated) and the viscous regimes of a shear flow of solid non-Brownian spheres in a viscous fluid, where the volume fraction of the particulates was high. The two most important features of the apparatus were: (a) a porous boundary that permitted liquid pressures to equilibrate and (b) a floating element of wall that was capable of measuring both shear and normal stresses. Under conditions of constant solid fraction, the transition from a strain rate independent stress to a linearly dependent one was found to occur with a local minimum in the stresses. The first direct measurements of the normal stress since 1954 demonstrate conclusively its existence even in the "viscous" regime where stresses scale linearly with strain rate.

Complementary experiments carried out at constant normal stress revealed a gradual increase in the solid fraction with strain rate, called viscous compaction, followed by dilatation. This leads to a maximum packing fraction that is not a constant as has been traditionally assumed but a function of the imposed normal stress. The initial compaction is believed to be a macroscopic manifestation of a transition in the internal microstructure due to the onset of viscous effects.

Acknowledgement—The authors wish to express their thanks to Mr Richard Fenner of the Fluid Mechanics Laboratory for his invaluable assistance in the design of these experiments.

REFERENCES

Bagnold, R. A. 1954 Experiments on a gravity-free dispersion of large solid spheres in a Newtonian fluid under shear. *Proc. R. Soc. Lond.* **225,** 49–63.

Brady, J. F. & Bossis, G. 1985 The rheology of concentrated suspensions of spheres in simple shear flow by numerical simulation. *J. Fluid Mech.* **155,** 105–129.

Brennen, C. E. & Pearce, J. C. 1978 Granular material flow in two-dimensional hoppers. *J. Appl. Mech.* **45,** 43–50.

Bridgewater, J. 1972 Stress–velocity relationships for particulate solids. ASME Paper 72-MH-21.

Buggisch, H. & Stadler, R. 1986 On the relation between shear rate and stresses in one-dimensional steady flow of moist bulk solids. *Proc. World Congress on Particule Technology*, Part III, Nurnberg, 16–18 April, 1986, pp. 187–202.

Campbell, C. S. & Brennen, C. E. 1985 Computer simulations of granular shear flows. *J. Fluid Mech.* **151,** 167–188.

Cheng, D. C.-H. & Richmond, R. A. 1978 Some observations on the rheological behavior of dense suspensions. *Rheol. Acta* **17,** 446–453.

Finney, J. L. 1970 Random packings and the structure of simple liquids I: the geometry of random close packing. *Proc. R. Soc. A* **319,** 479–493.

Frankel, N. A. & Acrivos, A. 1967 On the viscosity of a concentrated suspension of solid spheres. *Chem. Engng Sci.* **22,** 847–853.

Gadala-Maria, F. & Acrivos, A. 1980 Shear-induced structure in a concentrated suspension of solid spheres. *J. Rheol.* **24,** 799–814.

Hanes, D. M. & Inman, D. L. 1985 Observations of rapidly flowing granular materials. *J. Fluid Mech.* **150,** 357–380.

Hopkins, M. A. & Louge, M. Y. 1991 Inelastic microstructure in rapid flows of granular materials. *Phys. Fluids A* **3,** 47–57.

Hungr, O. & Morgenstern, N. 1984 High velocity ring shear tests on sand. *Geotechnique* **34,** 415–421.

Jenkins, J. T. & Savage, S. B. 1983 A theory for the rapid flow of identical smooth nearly elastic particles. *J. Fluid Mech.* **130,** 187–202.

Leighton, D. & Acrivos, A. 1987 The shear-induced migration of particles in concentrated suspensions. *J. Fluid Mech.* **181,** 415–439.

Nguyen, T. V., Brennen, C. E. & Sabersky, R. H. 1979 Gravity flow of granular materials in conical hoppers. *J. Appl. Mech.* **46,** 529–535.

Onoda, G. Y. & Liniger, E. G. 1990 Random loose packings of uniform spheres and the dilatancy onset. *Phys. Rev. Lett.* **64,** 2727–2730.

Pätzold, R. 1980 Die Abhängigkeit des Fliessverhaltens konzertrierter Kugelsuspensionen von der Strömungsform: ein Vergleich der Viskosität in Scher- under Dehnströmungen. *Rheol. Acta* **19,** 322–344.

Poutiatine, A. I. 1990 Dynamic shear cell for transient liquefaction and solidification of highly concentrated two-phase flows. M.Sc. thesis, Department of Mechanical Engineering, Massachusetts Institute of Technology, Cambridge, MA.

Prasad, D. 1993 Constitutive behavior and regime transition in dense suspensions at low strain rates. M.Sc. thesis, Department of Mechanical Engineering, Massachusetts Institute of Technology, Cambridge, MA.

Prasad, D. & Kytömaa, H. K. 1995 On the stability of rheometric systems used in the measurement of dense suspensions. *J. Fluids Engng.*

Reynolds, O. 1885 On the dilatancy of media composed of rigid particles in contact. *Phil. Mag.* **20,** 469–481.

Rutgers, R. 1962a Relative viscosity of suspensions of rigid spheres in Newtonian liquids. *Rheol. Acta* **2,** 202–210.

Rutgers, R. 1962b Relative viscosity and concentration. *Rheol. Acta* **2,** 305–348.

Savage, S. B. & McKeown, S. 1983 Shear stresses developed during rapid shear of concentrated suspensions of large spherical particles between concentric cylinders. *J. Fluid Mech.* **127,** 453–472.

Savage, S. B. & Sayed, M. 1984 Stresses developed by dry cohesionless granular materials sheared in an annular shear cell. *J. Fluid Mech.* **142,** 391–430.

Schofield, A. N. & Wroth, C. P. 1968 *Critical State Soil Mechanics.* McGraw–Hill, New York.

Scott, G. D. 1960 Packing of equal spheres. *Nature* **188,** 908–909.

Scott, R. F. 1963 *Principles of Soil Mechanics.* Addison–Wesley, Reading, MA.

Thomas, D. G. 1965 Transport characteristics of suspensions: VIII. A note on the viscosity of uniform spherical particles. *J. Colloid Sci.* **20,** 207–277.

Thompson, P. & Grest, G. 1991 Granular flow: friction and the dilatancy transition. *Phys. Rev. Lett.* **67,** 1751–1754.